

# Deployable Soft Composite Structures

Wei Wang<sup>1</sup>, Hugo Rodrigue<sup>1,2</sup> and Sung-Hoon Ahn<sup>1,2,†</sup>

<sup>1</sup>Department of Mechanical and Aerospace Engineering, Seoul National University, Seoul, Korea

<sup>2</sup>Institute of Advanced Machines and Design, Seoul National University, Seoul, Korea

<sup>†</sup>Corresponding author. [ahnsh@snu.ac.kr](mailto:ahnsh@snu.ac.kr)

## Materials and Methods

**Materials.** The SMA wires used for all prototypes are Flexibnol<sup>®</sup> (55wt% Ni, 45wt% Ti) from Dynalloy, Inc and their main properties are shown in Table S1. Polydimethylsiloxane (PDMS, Sylgard<sup>®</sup>184) from Dow Corning Corporation<sup>®</sup> is used as the polymeric matrix of all actuators and its main properties are shown in Table S2. Acrylonitrile butadiene styrene (ABS) is used for the embedded structure and mold of all actuators with the ABS parts being manufacturing by fused deposition modeling (FDM) machine using a Dimension 768 SST machine from Stratasys<sup>®</sup> Ltd. Electrically non-conductive polyimide (PI) tubes (D. Soar Green<sup>®</sup>, China) with an inner and outer diameter of 0.18 mm and 0.20 mm are used to cover the Ni-Cr wires and their main properties are shown in Table S3. Field's metal (32.5% Bi, 16.5% Ti, 51% In) from RotoMetals<sup>®</sup>, Inc is used as the phase changeable material and is melted in a beaker at temperature of 80°C in an environmental chamber (WTH-155, Daihan-brand<sup>®</sup>). Commercial Ni-chrome wires (Ni-Cr, 80 wt% Ni, 20 wt% Cr) are used to melt the fusible alloy.

**Control unit.** Through experimentation, the actuating currents for the 0.152 mm and 0.203 mm diameter SMA wires embedded in the SSC were determined to be 0.55 A and 1.0 A, respectively. The embedded FA structures are melted by applying a current of 1.0 A to the Ni-Cr wires for 40 s. A current control board connected to a CompactRIO 9024 embedded real-

**Table S1.** Material properties of SMA (Flexinol).

Parameter	Value
Martensitic Young's modulus	$E_{Mar}=28$ GPa
Austenitic Young's modulus	$E_{Aus}=75$ GPa
Martensitic start temperature	$M_S=77$ °C
Martensitic finish temperature	$M_f=42$ °C
Austenite start temperature	$A_s=81$ °C
Austenite finish temperature	$A_f=106$ °C
Wire diameter	152.4 $\mu$ m
Resistance per meter	55 $\Omega$
Initial strain	$\epsilon_0=5\%$

**Table S2.** Main properties of PDMS (Sylgard 184).

Parameter	Value
Useful temperature range	-45 to 200 °C
Specific gravity	1.03 @ 25 °C
Heat cure	8 hours @ 58 °C
PDMS Young modulus	$E_{PDMS}=1.8$ MPa (25 °C)
Thermal conductivity	0.27 W/m K
Volume Resistivity	$2.9 \times 10^{14}$ $\Omega$ -cm

**Table S3.** Material properties of PI tube (D. Soar Green).

Parameter	Value
Inner diameter	0.18 mm
Thickness	0.015 mm
Density	$1.41 \times 10^3$ kg/m <sup>3</sup>
Temperature limit	380 °C
Dielectric Strength	$>1.18 \times 10^{10}$ KV/m
Heat conductivity coefficient	$35.0 \times 10^{-5}$ °C/cm

time controller and a NI 9264 module (National Instruments, USA) is used to control the current applied to the SMA wires and the Ni-Cr wires, and Labview 2012 is used to input the current patterns. Using this experimental setup, the current patterns are set individually, including the actuation time and the magnitude of the currents for each channel.

**Bending modulus of actuator.** The variable stiffness property of the actuator structure shows a significant difference in stiffness with the solidified and the melted FA structure. In order to quantify this difference in stiffness, the flexural property of the actuator was measured using a three-point loading test according to the ASTM D 790-03 standard test method. The test was done using a span-to-depth ratio of 16:1 on a tensile testing machine (5948 MicroTester, Instron, US) with a 3-point flexure fixture (2810-400, Instron, US). The flexural modulus,  $E$ , of the specimens was calculated using the followed equation.

$$E = \frac{L^3 m}{4bh^3} \quad (1)$$

where  $L$  is the support span,  $m$  is the gradient of the load-displacement curve,  $b$  and  $h$  are the beam width and thickness.

**Assembling of deployable structures.** The deployable structures are assembled using mechanical revolving joints with the desired revolving motion range. To assemble a deployable triangular mast, nine basic hinge actuators form three modules, and the three modules are connected using shared platforms with mechanical revolving joints (Figure S1). To assemble a planar deployable structure, four basic hexagonal looping modules are connected to form an extended structure using two different kinds of mechanical joints (Figure S2). To assemble a ring deployable structure, six basic quadrilateral looping modules are connected to form an extended closing structure using passive mechanical joints with a revolution range of  $60^\circ$  (Figure S3).

**Experimental setup for deployable mirror.** To verify the effect of the light reflection, the deployable mirror is used to reflect sunlight onto a small-scale solar panel (50×60, mm) located in dark. A light-emitting diode (LED) is connected to the small-scale solar panel. When the sunlight is reflected onto the solar panel, the LED can be powered up. The LED is sealed in an aluminum square tube and the state of the LED is recorded from the other end of the tube (Figure S4). The experiments were conducted on August 27<sup>th</sup>, 2015 at 11:30 AM and the coordinates of the position where the experiments were conducted is (37.44961, 126.95257) at an altitude of 220 m. The temperature at the time of the experiments is 28°C and the humidity is 35%.

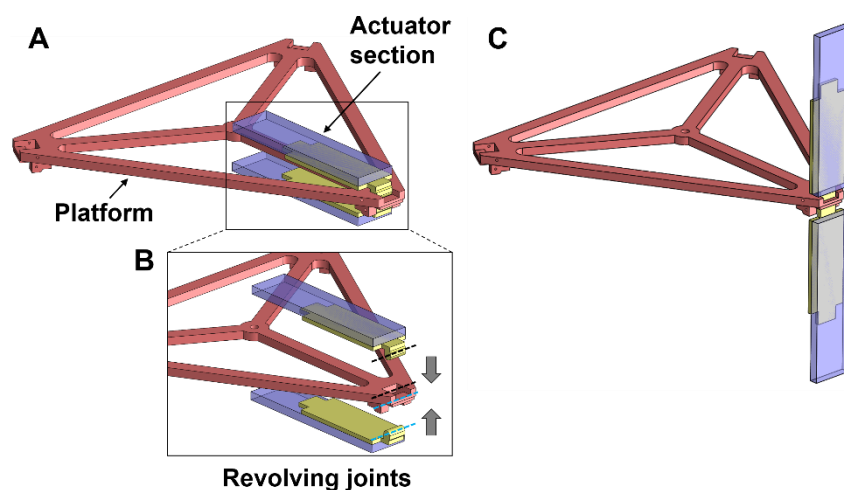


**Figure S1.** Assembly of triangular mast structure. (A) Folded state of the mast structure and (B) the components of the mechanical revolving joints. (C) Fully deployed configuration of the structure where the motion range of the mechanical hinge is 90 °.

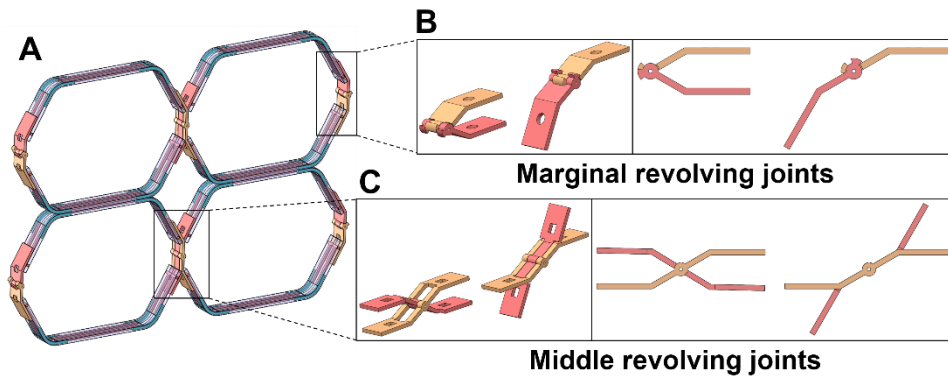


**Figure S2.** Assembly of planar deployable structure. (A) Schematic of the assembled planar structure with four hexagonal modules. (B) Oblique view and front view of the marginal revolving joints with a revolution range  $60^\circ$ . (C) Oblique view and front view of the middle revolving joints.

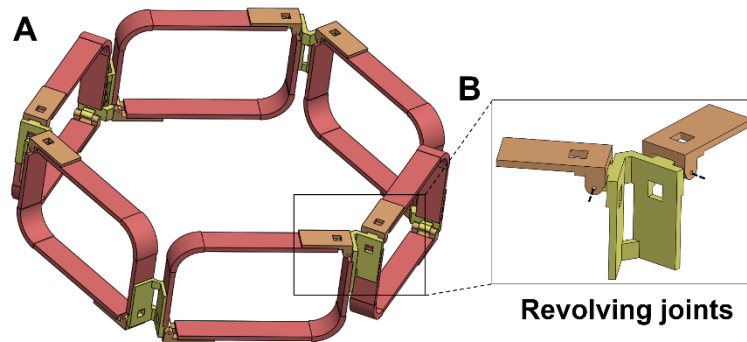


**Figure S3.** Assembly of ring deployable structure. (A) Schematic of the assembled ring structure with six quadrilateral modules. (B) The design of the revolving joints between each module where two joints are located at an angle of  $60^\circ$  with a revolving range  $90^\circ$  each.

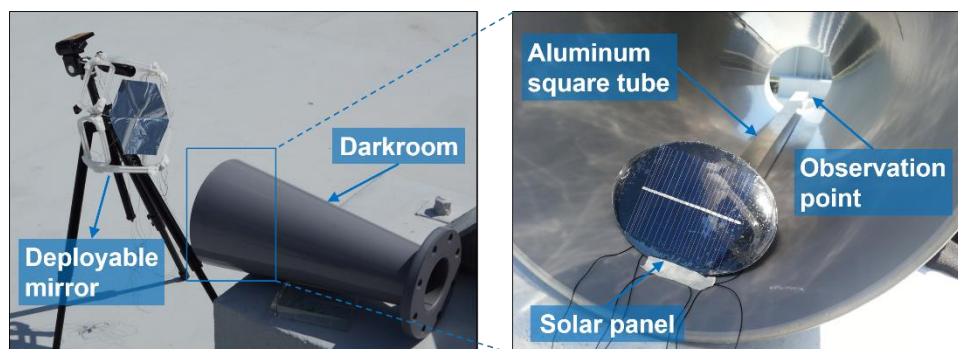


**Figure S4.** Experimental setup for testing the functionality of the proposed deployable mirror.

## **Supporting Videos**

**Video S1.** Unfolding process of a single actuator when its stiffness changes from the high stiffness state to the low stiffness state.

**Video S2.** Deploying processes of the folded triangular module structure and of the triangular mast comprising three modules in-line.

**Video S3.** Deploying processes of the hexagonal looping module and of the planar deployable structure composed of four hexagonal modules.

**Video S4.** Deploying processes of the quadrangular looping module and of the ring deployable structure composed of six quadrangular modules.

**Video S5.** Deploying process of the deployable mirror.